IMAV2017-26
https://www.imavs.org/pdf/imav.2017.26

Developing a Stable Small UAS for Operation in Turbulent Urban Environments

R. Gigacz*, A. Mohamed*, P. Poksawat, S. Watkins and A. Panta
RMIT University, Melbourne

ABSTRACT

The stability of Small Unmanned Air Systems (SUASs) can be challenged by turbulence during low-altitude flight in cluttered urban environments. This paper explores the benefits of a tandem wing aircraft configuration with the implementation of a pressure based phase-advanced turbulence sensory system on a SUAS for gust mitigation. The objective was to utilize passive and active methods to minimise gust-induced perturbations. Experimentation in repeatable turbulence within a wind tunnel's test section was conducted. The experiments focus on the roll axis, which is isolated through a specially designed roll-axis rig. The results shows improvement over conventional aircraft. This work is part of a larger research project aimed at enabling safe, stable and steady SUAS flight in urban environments.

1 INTRODUCTION

Small Unmanned Air Systems (SUASs), or Micro Air Vehicles (MAVs) typically operate at low altitude, within the atmospheric boundary layer. This region is optimum for a range of SUAS applications in Intelligence, Surveillance, and Reconnaissance (ISR) missions and is characterised as having high turbulence intensity [1, 2]. In the presence of winds, SUAS performance can degrade significantly [3]. However, turbulence poses an even greater threat to the vehicle's attitude stability [4–7]. Consequently, attitude control in turbulence is a critical issue for SUASs and MAVs as identified by Mohamed, Massey, Watkins and Clothier [8]. Current attitude control systems can be challenged by atmospheric turbulence [9]. Sensors which have the ability to detect the oncoming gusts could potentially complement or replace conventional inertial-based sensors for robust attitude control [10, 11]. Phase-advanced multi-hole pressure based sensors which are able to react to the turbulence ahead of the leading edge have been developed and patented [12], these have been shown to increase the stability of SUASs in turbulence [13].

This paper explores passive and active methods of aiding the stability of SUASs through experimental wind tunnel testing of a tandem wing airframe, in conjunction with the phase-advanced multi-hole pressure probes, to further enhance the attitude control performance in high levels of turbulence. Roll perturbations were identified as the most significant disturbing factor for small fixed-wing aircraft [1, 14] and consequently will be the focus of this paper.

2 TANDEM WINGS

The concept of a tandem wing aircraft is not a new one, Minardo and Trainelli [15] compiled a report with many examples of tandem wing aircraft which have been produced, noting how the first Wright Flyer in itself was partially a tandem wing, being a Canard configuration aircraft. A tandem wing aircraft is described as being an aircraft with two independent lift generating wings, which eliminates the need for a conventional horizontal tail and elevator. In order for it to remain a true tandem wing aircraft and not a canard aircraft, both wings must be of similar wingspans, and they will generally be set on different planes separated vertically and/or horizontally. It should be noted although many different civilian tandem wing aircraft have been built over time, the design has not become popular. In recent times the tandem wing configuration has started to make a resurgence, unmanned aircraft can potentially benefit from a tandem wing configuration and it has been implemented successfully in various aircraft (e.g., ADCOM Systems Yabhon, Aeronvironments Switch Blade and Innocons MicroFalcon).

There have been various studies on Low Reynolds number tandem wing airfoils, such as [16] along with [17] which primarily looked at optimization of a tandem wing design, but not in relation to flight through high levels of turbulence. The tandem wing configuration has a number of hypothesized advantages with respect to counteracting turbulence and when used in conjunction with the phase-advanced multi-hole pressure sensor system, as outlined in Figure 1. They are are well suited for precision active control through the control surfaces embedded in its wings providing higher control authority and an added degree of freedom (heave). Heave is a translational vertical movement up or down, which is created by activating both the control surfaces on the front and rear wings to an extent which would provide an equal lift on both sets of wings, thus creating a heave motion. Heave has been identified as a common perturbation for SUASs and MAVs when in turbulence with length scales that are greater or equal to its wing span [8,18]. The tandem wing design would appear to counter heave perturbations without the need to change the aircrafts pitch angle as much as is the case with conventional configu-

*Email address(es): Rohan.Gigacz@gmail.com, Abdulghani.Mohamed@rmit.edu.au

rations. This can be particularly useful for on-board payloads which can be blurred due to rotational motion. Furthermore, the implementation of advanced pressure sensors [10, 11, 13] on tandem wing designs has the potential to enhance the time advantage by allowing the placement of the roll control surfaces (ailerons) further aft of the probe sensors and enables a number of control architectures to be utilised.

3 Vehicular Development

A tandem wing aircraft has been developed (Figure 2 and 7) which utilises the phase-advanced multi-hole pressure sensors ahead of the front wings leading edge, as used in [13]. The specifications of the aircraft are outlined in Table 1 and 2. Due to the high frequency demands of stable flight in a high level of turbulence, high performance servos must be utilised for movement of the control surfaces. An all metal gear servo was selected, the metal gears are necessary to allow for sustained high frequency and load movement of the servos without overheating. Specifications of this servo are outlined in Table 3.

A fixed span, flat-plate airfoil was selected for the experimental aircraft, it's performance in smooth flow has has been documented by Mueller [19].

The sizing of the aircraft and its wings were made to be representative of typical SUASs which can be handled and launched by one person.

For the purpose of comparison, a fixed span flat-plate horizontal stabilizer of $40\ \%$ of the main wing was used. This additional horizontal stabiliser replaced the rear wing, to represent a similarly sized conventional aircraft of the same wing span. This conventionally winged alteration of the tandem wing SUAS is shown in Figure 3.

Characteristic	Detail
Airfoil	Flat plate
Leading Edge	Ellipsoid
Wing length	290.0 mm
Wing-span	650.0mm
Chord	150.0 mm
Camber	4.0 mm
Cruise speed	9 m/s
Wing spacing (LE - LE)	450 mm

Table 1: Aircraft specifications.

3.1 Control System

A custom developed flight controller was used to control the aircraft's attitude. The main components are a 32-bit ARM processor and an inertial-measurement-unit (IMU), which are required for the attitude estimation and real-time control implementation. A nonlinear complementary filter, presented in [20], is implemented to compute the aircraft's attitude. In addition to the conventional IMU based control architecture, the differential phase-advanced pressure based system as previously described is implemented to react to the turbulence ahead of the aircraft. This system has been outlined in [13] and is implemented by placing the differential pressure probes ahead of the leading edge of each of the front wings. The measured pressure is used as a feed-forward into the inner loop control system of the cascaded PID controller, as shown in Figure 4, where Kff is the feed forward gain to be tuned experimentally.

Component	Detail
Processor	Teensy 3.2
IMU	MPU6050
Servo	RJX FS0435HV
Receiver	FrSky XSR 2.4 Ghz ACCST
ESC	Turnigy 30 A, SBEC 4 A 5 V
Battery	Turnigy 1200 mah 25-50 C 3 S
Pressure Sensor	Honeywell HSCDRRN005NDAA3
Data Logger	"Blackbox" Data Recorder
Voltage Regulator	DC-DC Stepdown Module

Table 2: Aircraft component specifications.

Characteristic	Detail
Operating Voltage	4.8 - 7.4 V
Torque	3.4 kg/cm @ 7.4 V
Speed	0.04 sec/60° @ 7.4 V
Frequency	333 hz
Gear Type	All Metal Gear
Weight	20 g

Table 3: RJX FS0435HV servo specifications.

4 Experimental Setup

Passive turbulence generation, using planar grids, represented the most suitable method for producing elevated levels of turbulence intensity inside a wind tunnel. RMITs Industrial Wind-Tunnel (2x3x9 m test section) was considered sufficiently large to simulate the relevant turbulence conditions of varying length scales and intensities, the aircraft in the tunnel with the turbulence grid can be seen in Figure 2 and 7. The approach outlined by Watkins, et al [21] is followed to characterize SUAS's and MAV's flight environment and replicate atmospheric turbulence. A Reynolds Number of $\approx$ 60,000 was tested representing typical SUAS flight regime. The selected turbulence intensities were $12.6\ \%$ and $18.0\ \%$ with a length scale of $0.31\ m$. The wind tunnel was operated at a speed which corresponds to $9\ m/s$ at the aircraft's position, this airspeed value representative of typical SUAS and MAV flight speeds.

The primary focus of this paper is comparing the roll stability characteristics of the tandem wing aircraft with the

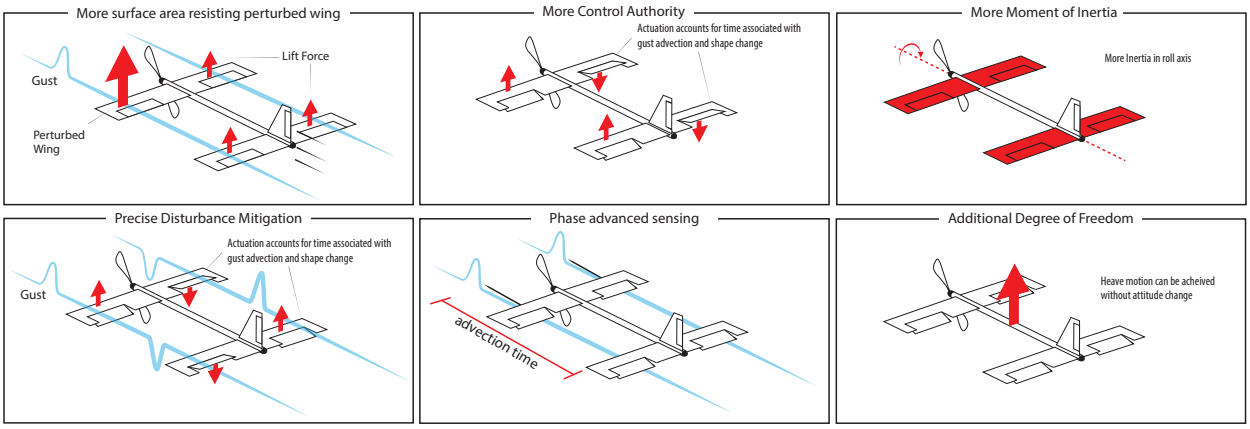

Figure 1: Tandem wing aircraft hypothesized advantages with respect to counteracting turbulence.

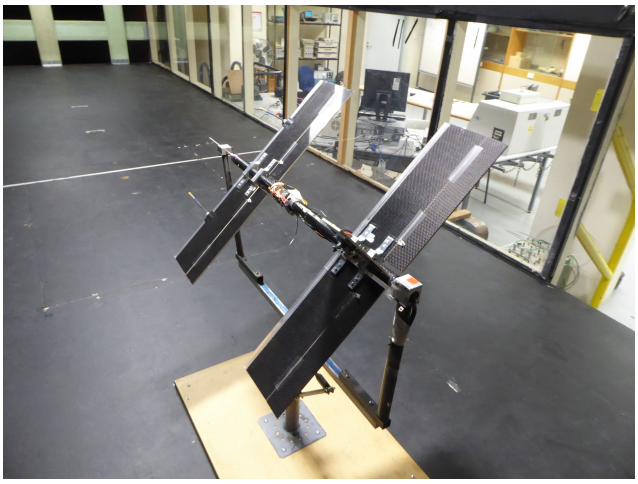

Figure 2: Tandem wing SUAS in roll rig.

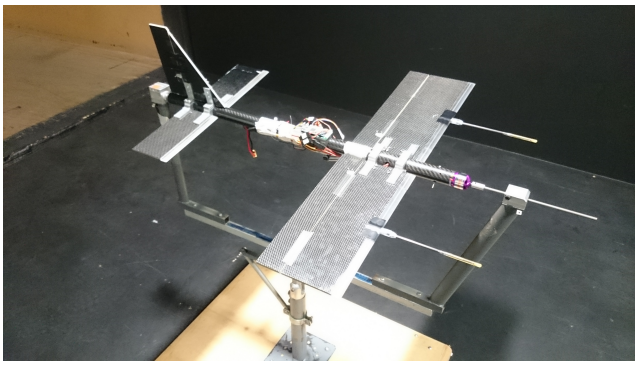

Figure 3: Conventional SUAS in roll rig.

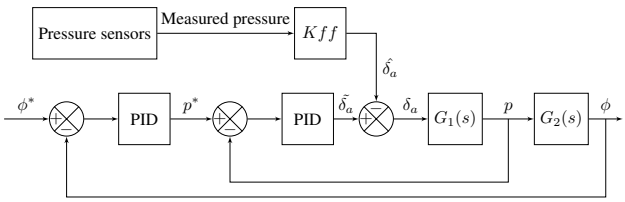

Figure 4: Pressure-based cascaded PID control structure for the roll axis.

pressure probes either active or inactive, with both the front and rear wing control surfaces acting as ailerons. Although for real flight of a tandem wing aircraft, the front wing may generally have a higher loading with the CG towards the front wing and thus some trim to the control surfaces would be needed, this study looks at the system with all control surfaces trimmed at a 0°angle.

The aircraft's roll performance has been assessed through the aid of the roll axis rig detailed in [22]. The rig constrains the motion of the SUAS to a single axis, that of roll, with low friction.

4.1 Aircraft Control Loop Tuning

The roll axis PID gains were tuned in the selected experimental turbulence level of 12.6 % via a process of trial and error, where the final selection of each gains value was selected by running the aircraft for 60 seconds over a range of estimated gain values, and analysing the resulting data, with the value selected which corresponded to the least roll angle and roll rate perturbations. As this is a SUAS operating in high frequency turbulence the Derivative component of the PID controller is neglected, this is because the derivative term amplifies noisy signals [23]. This can also be better for the servos, as it may reduce the demand placed on them by reducing the frequency of actuation commands. Only the Proportional and Integral components of the PID control loop are needed.

Probability density functions (PDF) and boxplots were used to analyse the aircraft's performance while tuning in terms of roll angle and roll rate. The boxplot is a typical box and whiskers plot with a line for the median, '+' for the mean, a box around the 25 % and 75 % quartiles and whiskers bounding 2.5 % and 97.5 %. The PDF plots can be interpreted such that a lower distribution and higher peaks corresponds to a reduction in perturbations of roll angles and roll rates.

A similar process of trial and error was followed when tuning the pressure sensor control loop gains, Kff. An example of this tuning is shown through PDFs and boxplots in Figure 5 and 6, whereby the Kff value of 25 was initially selected as the most appropriate value as it corresponded to the least roll angle and roll rate perturbations. After this initial range was tested, the range of values were further lowered until a more precise value was obtained.

A similar process was followed for the conventional aircraft, however only the rate mode PID gains required change, with the attitude mode and probe gains able to remain the same.

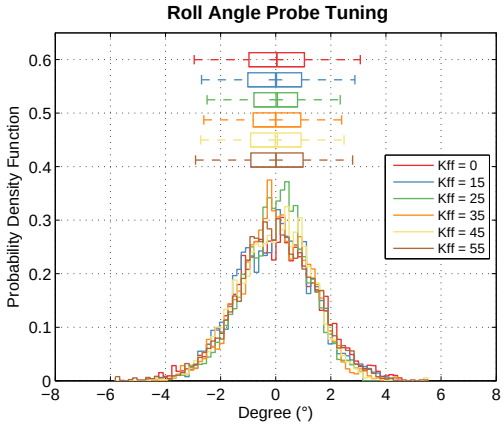

Figure 5: Roll angle probe tuning.

5 Results

PDFs and boxplots were used to analyse the aircraft's stability performance, where if the aircraft remained completely unperturbed in roll, the PDF plot would all be at 0°. Figure 8 and 9 show a comparison of the perturbations of the tandem wing and conventional aircraft in 12.6 % turbulence intensity, with and without the pressure probe system activated in the control loop. It can be seen through the smaller box plots, higher peaks and lower distribution that there is a reduction in perturbations when the pressure probes are activated for both the tandem wing and conventional aircraft. Through similar analysis of the PDFs and boxplots, it can be observed that the tandem wing aircraft has lower perturbations in the turbulence compared to the conventional aircraft.

In an effort to further explore the tandem wing aircraft's stability performance in high levels of turbulence, testing was

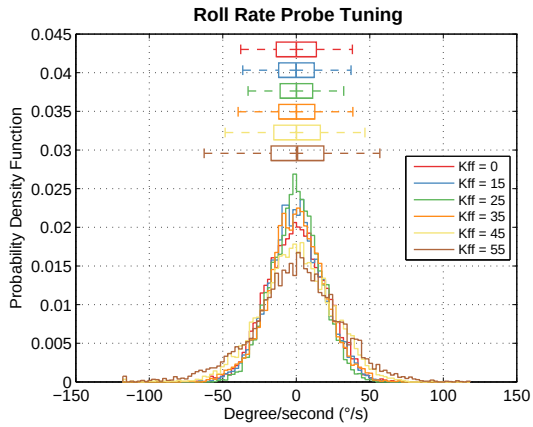

Figure 6: Roll rate probe tuning.

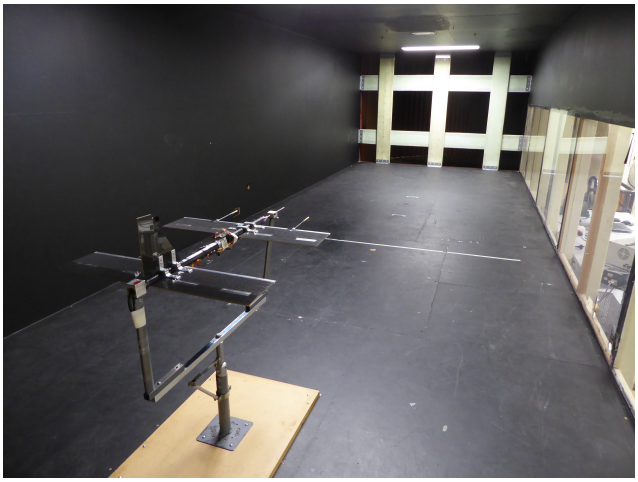

Figure 7: Tandem wing SUAS in roll rig.

conducted in 18 % turbulence intensity. PDFs and box plots of the aircraft's performance at this intensity are shown in Figure 10 and 11. Much like in 12.6 % turbulence intensity, there is a reduction in perturbations when the pressure probes were activated.

6 Conclusion

A tandem wing SUAS has been developed that is equipped with phase-advanced multi-hole pressure sensors to explore means of improving the attitude control in high levels of turbulence. Baseline performance and performance improvements have been demonstrated, emphasising the suitability of the tandem wing configuration in aiding safe and stable SUAS flight in turbulent urban environments. Much like past studies with conventional aircraft, utilising the phase-advanced pressure probes in conjunction with a standard PID control structure improves the roll stability of tandem wing SUASs in turbulence. Furthermore it has been

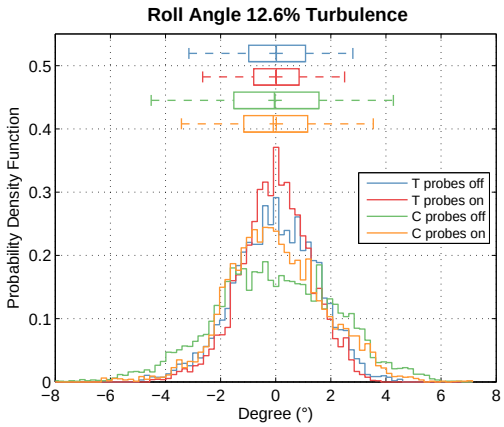

Figure 8: Roll angle perturbation of tandem wing (T) & conventional (C) aircraft with pressure probes off and on in 12.6 % turbulence intensity.

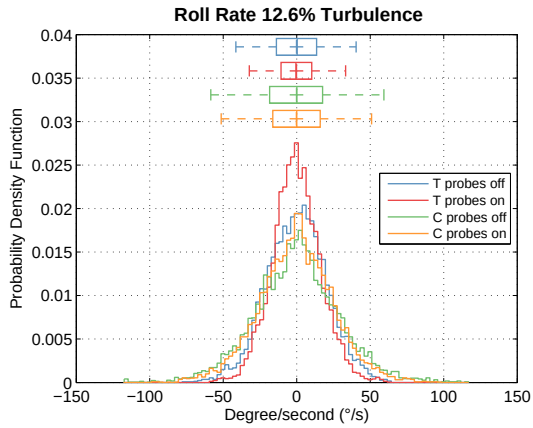

Figure 9: Roll rate perturbation of tandem wing (T) & conventional (C) aircraft with pressure probes off and on in 12.6 % turbulence intensity.

demonstrated that a tandem wing aircraft has lower roll angle and roll rate perturbations than a conventional aircraft with the same wing span in 12.6 % turbulence intensity. Future work will explore varying control architectures and configurations, comparisons with different conventional aircraft set ups, along with testing without the aid of a roll rig, including testing of the tandem wing configuration heave and pitch characteristics in turbulence.

Acknowledgements

The authors wish to acknowledge the technical support provided by Gilbert Atkins at RMIT University for setting up the experimental instruments in order to conduct the presented research. This research was undertaken as part of the RMIT Unmanned Aircraft Systems Research Team, within the Sir Lawrence Wackett Aerospace Research Centre, at RMIT University. This work has been partially funded and supported in part by; the U.S. Air Force Office for Scientific Research (AFOSR); Defence Science and Technology Group (DSTG); Defence Science Institute (DSI); and the Australian Government Research Training Program Scholarship.

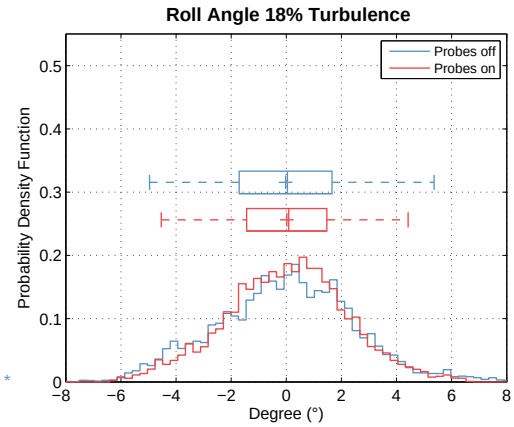

Figure 10: Roll angle perturbation of tandem wing aircraft with pressure probes off and on in 18 % turbulence intensity.

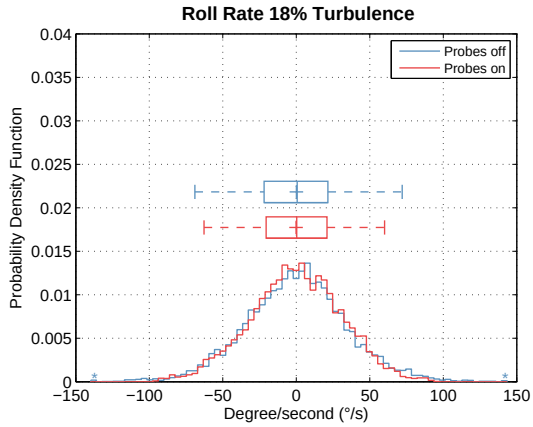

Figure 11: Roll rate perturbation of tandem wing aircraft with pressure probes off and on in 18 % turbulence intensity.

References

[1] S. Watkins, J. Milbank, and B. J. Loxton, "Atmospheric Winds and their Implications on Micro Air Vehicles," *AIAA journal*, no. September, 2006.

[2] S. Watkins, M. Thompson, B. Loxton, and M. Abdulrahim, "On Low Altitude Flight Through The Atmospheric Boundary Layer," *International Journal of Micro Air Vehicles*, vol. 2, no. 2, pp. 55–68, 2010.

[3] C. White, S. Watkins, E. W. Lim, and K. Massey, "The Soaring Potential of a Micro Air Vehicle in an Urban

Environment," *International Journal of Micro Air Vehicles*, vol. 4, no. 1, pp. 1–14, 2012.

[4] C. R. Galinski, "Gust Resistant Fixed Wing Micro Air Vehicle," *Journal of Aircraft*, vol. 43, no. 5, pp. 1586–1588, 2006.

[5] C. Galinski and R. Zbikowski, "Some problems of micro air vehicles development," *Bulletin of the Polish Academy of Sciences-Technical Sciences*, vol. 55, no. 1, pp. 91–98, 2007.

[6] P. Lissaman, "Effects of Turbulance on Bank Upsets of Small Flight Vehicles," *AIAA Aerospace Sciences Meeting Including The New Horizons Forum and Aerospace Exposition*, no. January, pp. 1–10, 2009.

[7] W. Shyy, H. Aono, S. K. Chimakurthi, P. Trizila, C.-K. Kang, C. E. Cesnik, and H. Liu, "Recent progress in flapping wing aerodynamics and aeroelasticity," *Progress in Aerospace Sciences*, vol. 46, no. 7, pp. 284–327, 2010.

[8] A. Mohamed, K. Massey, S. Watkins, and R. Clothier, "The attitude control of fixed-wing MAVS in turbulent environments," *Progress in Aerospace Sciences*, 2014.

[9] A. Mohamed, S. Watkins, R. Clothier, M. Abdulrahim, K. Massey, and R. Sabatini, "Fixed-wing MAV attitude stability in atmospheric turbulence-Part 1: Suitability of Conventional Sensors," *Progress in Aerospace Sciences*, 2014.

[10] S. Watkins, A. Mohamed, A. Fisher, R. Clothier, R. Carrese, and D. Fletcher, "Towards autonomous MAV soaring in cities: CFD simulation, EFD measurement and flight trials," *International Journal of Micro Air Vehicles*, vol. 7, no. 4, pp. 441–448, 2015.

[11] A. Mohamed, S. Watkins, R. Clothier, M. Abdulrahim, K. Massey, and R. Sabatini, "Fixed-wing MAV attitude stability in atmospheric turbulence-Part 2: Investigating biologically-inspired sensors," *Progress in Aerospace Sciences*, 2014.

[12] A. Mohamed, S. Watkins, and R. CLOTHIER, "Methods and systems for attenuating the effects of turbulence on aircraft," Dec. 3 2015, wO Patent App. PCT/AU2015/000,326. [Online]. Available: https://www.google.com/patents/WO2015179905A1?cl=en

[13] A. Mohamed, M. Abdulrahim, S. Watkins, and R. Clothier, "Development and Flight Testing of a Turbulence Mitigation System for MAVs," *Journal of Field Robotics*, pp. 1–22, 2015.

[14] M. Abdulrahim, S. Watkins, M. Thompson, R. Segal, M. Shortis, and J. Sheridan, "Measurements of Gust Sensitivity on MAVs: Part2," *AIAA Guidance, Navigation and Control*, 2009.

[15] A. Minardo, "The Tandem Wing: Theory, Experiments, and Practical Realisations," Ph.D. dissertation, 2014.

[16] D. F. Scharpf and T. J. Mueller, "Experimental study of a low Reynolds number tandem airfoil configuration," *Journal of aircraft*, vol. 29, no. 2, pp. 1–6, 1992. [Online]. Available: http://arc.aiaa.org/doi/pdf/10.2514/3.46149

[17] Z. Husain, M. Abdullah, and T. Yap, "Two-dimensional analysis of tandem/staggered airfoils using computational fluid dynamics," ... *Journal of Mechanical* ..., vol. 33, no. 3, 2005. [Online]. Available: http://manchester.metapress.com/index/X10L92T311420555.pdf

[18] R. C. Michelson., "Overview of micro air vehicle system design and integration issues," *Encyclopedia of Aerospace Engineering*, 2010.

[19] T. Mueller, "Aerodynamic measurements at low reynolds number for fixed wing micro-air vehicles." 2000.

[20] M. Euston, P. Coote, R. Mahony, J. Kim, and T. Hamel, "A complementary filter for attitude estimation of a fixed-wing UAV," *2008 IEEE/RSJ International Conference on Intelligent Robots and Systems, IROS*, pp. 340–345, 2008.

[21] S. Watkins, A. Fisher, A. Mohamed, M. Marino, M. Thompson, R. Clothier, and S. Ravi, "The Turbulent Flight Environment Close to the Ground and Its Effects on Fixed and Flapping Wings at Low Reynolds Number," *5th European Conference for Aerospace Sciences (EUCASS)*, pp. 1–10, 2013.

[22] A. Mohamed, S. Watkins, R. Clothier, and M. Abdulrahim, "Influence of Turbulence on MAV Roll Perturbations," *International Journal of Micro Air Vehicles*, vol. 6, no. 3, pp. 175–190, 2014.

[23] P. Poksawat, L. Wang, and A. Mohamed, "Automatic tuning of attitude control system for fixed-wing unmanned aerial vehicles," *IET Control Theory & Applications*, vol. 10, no. 17, pp. 2233–2242, 2016.